Residual aperiodic stochastic resonance in a bistable dynamic system transmitting a suprathreshold binary signal

Fabing Duan,* David Rousseau, and François Chapeau-Blondeau†
Laboratoire d'Ingénierie des Systèmes Automatisés (LISA), Université d'Angers, 62 avenue Notre Dame du Lac, 49000 Angers, France
(Received 27 June 2003; revised manuscript received 13 October 2003; published 30 January 2004)

Conventional stochastic resonance can be viewed as an amplitude effect, in which a small (subthreshold) input signal receives assistance from noise to trigger a stronger response from a nonlinear system. We demonstrate another mechanism of improvement by the noise, which is more of a temporal effect. An intrinsically slow system has difficulty to respond to a fast (suprathreshold) input, and the noise plays a constructive role by spurring the system for a more efficient response. The possibility of this form of stochastic resonance is established and studied here in a double-well bistable dynamic system, driven by a suprathreshold random binary signal, with the noise accelerating the switching between wells.

DOI: 10.1103/PhysRevE.69.011109 PACS number(s): 05.40.Ca, 05.45.−a

I. INTRODUCTION

Stochastic resonance (SR) is a phenomenon in which the response of a nonlinear system to a *subthreshold* periodic input signal is optimized by a nonzero level of noise [1–5]. The phenomenon of SR can be extended to cases with aperiodic broadband signals, that is, aperiodic stochastic resonance (ASR) [6,7]. For the bistable dynamic system used as a prototype model of SR, the term of subthreshold denotes the condition where the input signal amplitude is less than the critical value that just destroys the system bistability [4]. It is well known in these systems that for *suprathreshold* signals, conventional SR usually disappears [8–11]. This result has been established in many situations, including computational models [8,9], real neurophysiological studies [10], arrays of noisy Hodgkin-Huxley neurons [11]. Beyond, a residual SR effect was observed by Apostolico *et al.* [12] in a single bistable system subject to a suprathreshold sinusoidal signal. This residual SR is related to a synchronization-loss mechanism (resonant trapping) [12]. An observation of such a resonant trapping effect was also obtained in noise activated nonlinear dynamic sensors when measured by residence time distribution [13]. Stocks and co-workers [14–17] also introduced another form of SR, termed suprathreshold SR, which occurs in a parallel array of threshold devices or neuronal models with a predominantly suprathreshold input. Suprathreshold SR is then suggested as a coding strategy for sensory neurons [17]. This strategy is associated with recent experiments [18,19], which show that the coding of formant information in cochlear implants can be improved by adding noise to some suprathreshold stimuli. Additionally, it is interesting to note that the intrinsic receptor noise can enhance the encoding of small yet suprathreshold amplitude modulations by perturbing periodic phase locked patterns [20]. These results indicate that, in addition to subthreshold signal enhancement previously reported [1–11], noise can also play a constructive role to transmit suprathreshold signals through nonlinear systems [12–20].

In this paper, an ASR phenomenon is observed to survive in a *single* bistable dynamic system subject to a suprathreshold random binary signal. This form of suprathreshold ASR is distinct from the previous form of Ref. [12], in the input signal, and in the measure of performance receiving improvement from the noise. We term this effect residual ASR (suprathreshold). Generally, conventional ASR (subthreshold) [6] is more like an amplitude effect, wherein a small aperiodic input has an amplitude too small to trigger transitions at the output, and it gets assistance from noise for that. In contrast to conventional ASR, residual ASR (suprathreshold) as we will show is a temporal effect, wherein a slow dynamic system has difficulty to follow the variations imposed by a fast (suprathreshold) input, and it gets spurred by the noise for that. Other types of action of the noise on the response times of a bistable dynamic system have been observed, for instance in Ref. [21], where it is shown that the correlation duration of the noise associated to a sinusoidal forcing can have an impact on the distribution of hysteretic transition times at the output. Here, we will demonstrate that the temporal action of the noise can lead to an enhancement of information transmission from a fast suprathreshold input by addition of noise. However, as we will see, the input signal has to remain a little suprathreshold, but not too much, otherwise the positive effect of noise tends to vanish, whence our term ''residual.'' Residual ASR effects may be significant in bistable electronic or optical devices, where noise can be utilized in a constructive way as an aid to suprathreshold signal transmission. We also suggest that residual ASR effects may be of importance to biological systems, especially in situations where the system switching characteristic time cannot be neglected.

The paper is organized as follows: Section II introduces the bistable dynamic system under study. Considering the input information-bearing binary signal, the measure of the system performance is chosen as the bit error rate (BER). In Sec. III, an essential parameter for the existence of the residual ASR, the system switching time, is introduced. It is observed in numerical simulations that the bistable system subject to a random binary suprathreshold signal presents a (local) minimum in the BER at an optimal nonzero noise intensity, this being the residual ASR effect. This effect is

*Electronic address: fabing.duan@univ-angers.fr
†Electronic address: chapeau@univ-angers.fr

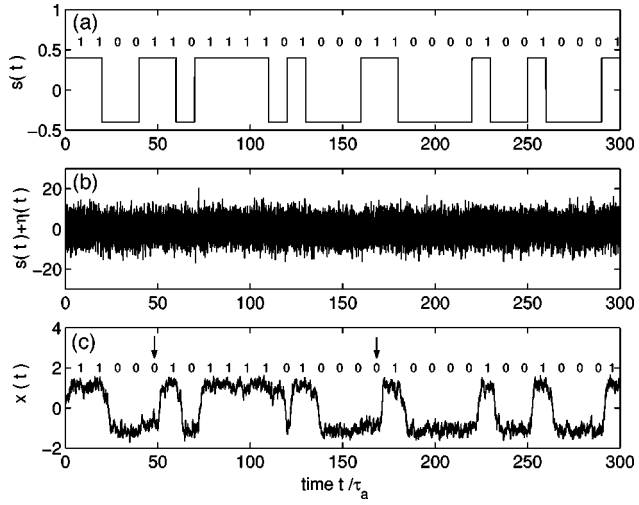

FIG. 1. Time evolution of the signals for the system of Eq. (1) with $\tau_a=1$ and $X_b=1$. (a) The random binary input signal $s(t)$ with $A=0.4$ and $T_p=10$. The corresponding source digits are also inset; (b) the mixture of signal $s(t)$ plus noise $\eta(t)$ with $D=0.1$ (in units $\tau_a X_b^2$); (c) The system state $x(t)$. According to the sampled values of $x(t)$ at $t_j=jT_p$ for $j=1,2,\ldots$, the readout digits are given in the inset. The erroneous digits are denoted by arrows. The sampling time step $\Delta t=0.01$.

discussed in detail by comparing the signal pulse duration to the system switching time. In Sec. IV, the mechanism of residual ASR effect is theoretically analyzed. An approximate theory based on a nonstationary probability density model is proposed. Finally, the conclusions are drawn and some further research directions are suggested.

II. BINARY SIGNAL TRANSMISSION BY A BISTABLE SYSTEM

In this paper, the input is a baseband binary pulse amplitude modulation signal [22]. In such a random signal, wave form $s_1(t)=+A$ represents digit 1 and digit 0 is mapped into wave form $s_2(t)=-A$, within a time interval of T_p. Here, A is the pulse amplitude and T_p is the pulse duration [22]. This kind of random binary signal $s(t)$, depicted in Fig. 1(a), has already been employed in both experimental evidences of binary ASR phenomenon [23,24] and numerical studies [25,26]. $s(t)$ is then corrupted by an additive Gaussian white noise $\eta(t)$ with autocorrelation $\langle \eta(t)\eta(0)\rangle=2D\delta(t)$ and zero mean. D denotes the noise intensity. Next, the mixture of signal and noise is applied to a bistable dynamic system given as [25]

$$\tau_a \frac{dx(t)}{dt}=x(t)-\frac{x^3(t)}{X_b^2}+s(t)+\eta(t), \tag{1}$$

with system parameters $\tau_a>0$ and $X_b>0$. τ_a is related to the system relaxation time. The dynamics of Eq. (1) is derived from the symmetrical double-well potential $V_0(x)=-x^2/2+x^4/(4X_b^2)$, having the two minima $V_0(\pm X_b)=-X_b^2/4$. Parameters τ_a and X_b have the units of time and signal amplitude, respectively, and define natural scales associated to the process of Eq. (1).

We are interested in recovering the successive input digits 0 and 1, from the observation of the system state $x(t)$. Input source digits represented by wave forms $s_i(t)$ for $i=1,2$ are emitted at a rate of one wave form every T_p and last over a duration T_p. To obtain the decoded digits, the system state $x(t)$ is sampled at equispaced times $t_j=jT_p$ for $j=1,2,\ldots$, resulting in a sequence of sampled values $x_j=x(t_j)$. Then, each x_j is compared to the decision threshold ℓ for decoding digit 0 or 1: If $x_j>\ell$, the decoded digit is 1, otherwise it is 0, as depicted in Fig. 1(c). In this communication process, we assume that the interval T_p at which input digits are emitted, and the transition times at which one given pulse of duration T_p ends while the next pulse starts at the emitter, are both known at the receiver. This is a case of synchronized communication, as considered in Ref. [25]. The times t_j of output readings are placed, as in Ref. [25], just at the end of one emitted pulse, just before the next pulse starts, this to maximize the time allowed for the state $x(t)$ to approach the stable state associated to the digit being currently transmitted.

Now, this system of Eq. (1) with input binary digits and output binary readings can be viewed as an information channel transmitting binary data. It has been analyzed as a memoryless symmetric binary channel in Refs. [25,26]. An information measure, the BER, will be used to quantify the performance of this nonlinear information channel. We assume that the input binary digits occur with equal probabilities, i.e., $P(0)=P(1)=1/2$, and are statistically independent. $P(0)$ and $P(1)$ represent the probabilities of digits 0 and 1 at the input, respectively. In the presence of noise, $P(0|1)$ is the probability of error for the decoded output to be 0 when the input digit is 1, and conversely for $P(1|0)$. Thus, the total probability of error P_e reads

$$P_e=P(0)P(1|0)+P(1)P(0|1). \tag{2}$$

Since each erroneous output digit will lose one bit of information [e.g., Fig. 1(c)], P_e is also called the BER in binary data transmission.

In this paper, we numerically integrate the stochastic differential equation of Eq. (1) using a Euler-Maruyama discretization method with a small sampling time step $\Delta t \ll \tau_a$ [27]. The block scheme for transmitting binary data by this nonlinear system of Eq. (1) has been designed in Ref. [26], wherein the input signal is generated by a pseudorandom binary signal generator. With this designed block scheme, the BER can be automatically recorded in numerical simulations.

III. RESIDUAL APERIODIC STOCHASTIC RESONANCE

In this section, the residual ASR effect is demonstrated in numerical simulations. An essential parameter which controls the residual ASR is the switching time of the dynamic system. Residual ASR will take place when this switching time is large in comparison to the repetition period T_p of the input bit stream.

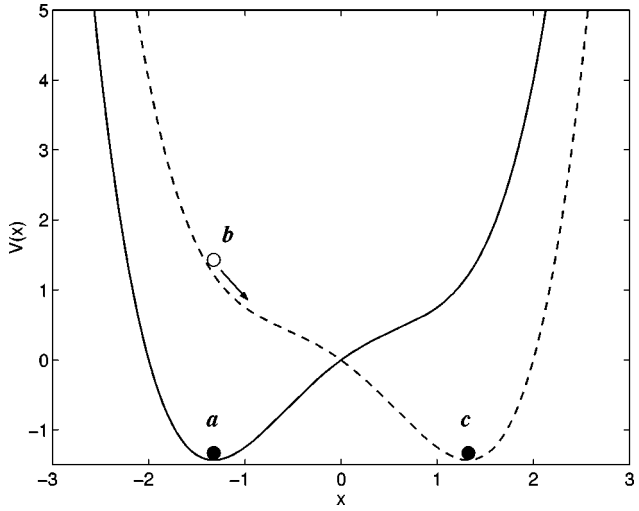

FIG. 2. Evolution of the potential function $V(x)$ and the explanation of the system switching. Stable positions ***a*** and ***c*** are the minima of the potential functions. States $x(t)$ at positions ***a*** and ***c*** are the real roots of the cubic equation $x-x^3/X_b^2 \mp A=0$. ***b*** is an unstable position. $\tau_a=1$, $X_b=1$, $A=1$, and $A_c \approx 0.38$.

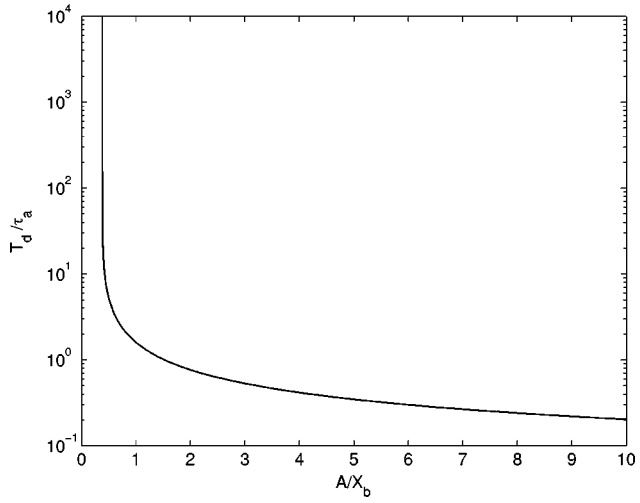

FIG. 3. Plot of the reduced switching time T_d/τ_a of Eq. (4) as a function of the reduced input amplitude A/X_b. The decision threshold $\ell=0$. Note that T_d/τ_a will tend to infinity as A/X_b approaches $A_c/X_b=2/\sqrt{27}$.

A. System switching time

The system switching time is the time taken by the system to switch from one potential well to the other, when the input signal switches from the amplitude $-A$ to $+A$ (or conversely). In the absence of the noise $\eta(t)$, the minimal value of the signal amplitude A that destroys the system bistability in Eq. (1), occurs when the cubic equation $x-x^3/X_b^2+A=0$ ceases to have three real roots. The outcome is that bistability is destroyed when $A>A_c=2X_b/\sqrt{27}\approx 0.38X_b$ [4,25].

In the absence of noise and $A>A_c$, if the system is modulated by the wave form $s_2(t)=-A$ for a sufficiently long time, the current internal state $x(t)$ resides at the stable position ***a***, i.e., the minimum of potential function $V(x)=-x^2/2+x^4/(4X_b^2)+Ax$ (see Fig. 2). Next, when the wave form $s_1(t)=+A$ is applied, $x(t)$ will be located at an unstable position ***b*** of the potential function $V(x)=-x^2/2+x^4/(4X_b^2)-Ax$. Progressively, $x(t)$ will tend towards the corresponding stable position ***c***, as shown in Fig. 2.

In this transition process, the switching time T_d is defined as the time for the system to evolve from the position ***b*** to the position defined by the decision threshold ℓ. An appropriate choice for this threshold, which preserves the symmetric character of the information channel, and which is adopted in the sequel, is $\ell=0$.

From Eq. (1) with no noise $\eta(t)$, we have

$$\frac{dt}{\tau_a}=\frac{dx}{x-x^3/X_b^2 \pm A}. \tag{3}$$

Therefore, the switching time T_d verifies

$$\frac{T_d}{\tau_a}=\int_{x_-}^{0}\frac{dx}{x-x^3/X_b^2+A}=C_1\ln\left[\frac{x_+}{x_+-x_-}\right]+C_2\ln\left[\frac{x_1}{x_1-x_-}\right]+C_3\ln\left[\frac{x_2}{x_2-x_-}\right], \tag{4}$$

where x_- is the unique real root of equation $x-x^3/X_b^2-A=0$ $(A>A_c)$. Similarly, x_+ is the unique real root of equation $x-x^3/X_b^2+A=0$, with two corresponding conjugate complex roots x_1 and x_2. C_1, C_2, and C_3 are integration constants. Theoretical expressions of x_-, x_+, x_1, x_2, C_1, C_2, and C_3 are developed in detail in Appendix A. This case is for the input signal amplitude varying from $-A$ to $+A$, but thanks to the symmetry of the process, the switching time T_d is the same when the input changes from $+A$ to $-A$.

In the present problem, τ_a can be taken as the unit of time, and X_b as the unit of signal amplitude. Parameters τ_a and X_b can be thought of as fixed and imposed by the transmission channel. What is important then is to investigate the influence of the parameters T_p and A attached to the input signal, and D attached to the noise. Our regime of interest for A here is $A>A_c=2X_b/\sqrt{27}$, i.e., a regime of suprathreshold input. By contrast, previous studies have considered the case of $A<A_c$ to show a form of stochastic resonance or a constructive role of the noise in binary signal transmission [25,26]. Equation (4) gives the switching time T_d in units of τ_a, and T_d is displayed in Fig. 3. We shall then study the interplay between a large T_d (slow system) in relation to a small T_p (fast input), and show that in such conditions, addition of noise via an increase of D can also play a constructive role.

B. Residual ASR phenomenon

A numerical simulation of the system of Eq. (1) has been undertaken, with the evaluation of the BER. The anticipated

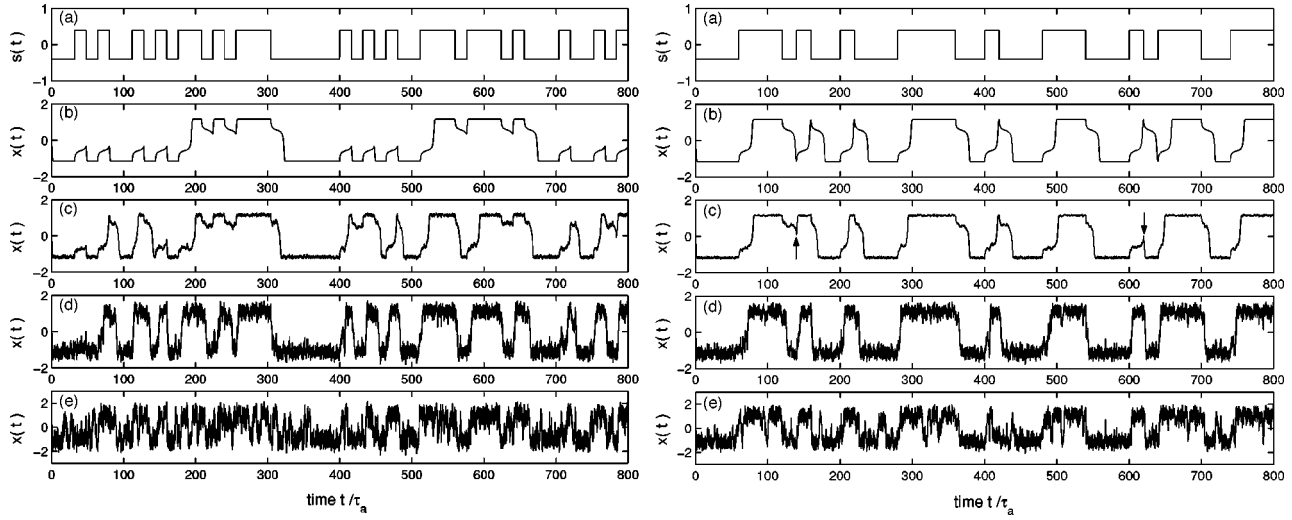

FIG. 4. Numerical results of time evolution of the signals for the system of Eq. (1) with $\tau_a=1$ and $X_b=1$ and $A/X_b=0.4$. D is in units $\tau_a X_b^2$. The sampling time step $\Delta t=0.01\tau_a$. Left: $T_p=16<T_d=17.5897$. (a) The input signal $s(t)$; The system output $x(t)$ with (b) $D=0$, (c) $D=0.005$, (d) $D=0.12$, and (e) $D=0.5$. Right: $T_p=20>T_d=17.5897$. (a) the input signal $s(t)$; the system output $x(t)$ with (b) $D=0$, (c) $D=0.002$, (d) $D=0.1$, and (e) $D=0.3$.

ASR effect with a fast input (small T_p) and a slow system (large T_d) is indeed observed.

Figure 4 (left) and (right) show two numerical examples of the time evolution of the signals for the system of Eq. (1), illustrating the essential features of the residual ASR effect at $T_p<T_d$ and $T_p>T_d$. When the suprathreshold input signal is fast (T_p is smaller than T_d), the system output cannot reach the decision threshold ℓ in one pulse duration of T_p [see, Fig. 4 left (b)]. In such a condition, the noise plays a constructive role, by spurring the output switchings of the system, helping them to better follow the transitions present in the fast suprathreshold input [see Fig. 4 left (d)]. This outcome confirms the prediction of the residual ASR effect with a fast input on a slow system ($T_p<T_d$). However, the condition $T_p<T_d$ for the occurrence of the residual ASR effect should not be taken as a strict quantitative condition. T_d is a strict measure of the switching time of the system only in the absence of noise; when noise is added, T_d is only an indicative measure of the switching time of the system. This is why, as shown in Fig. 4 right, the residual ASR effect can still survive when T_p is slightly above T_d. In Fig. 4 right, without the noise, the system output does cross the decision threshold ℓ in one pulse duration T_p [see Fig. 4 right (b)], providing error-free output digits with the decoding scheme introduced in Sec. II. With a small amount of noise at $D=0.002$, we observe that the switching of the system output can be, on some occasions, retarded by the noise, giving rise to some erroneous output symbols [see arrows in Fig. 4 right (c)]. On adding more noise, this possibility of retardation becomes ineffective [see Fig. 4 right (d) and (e)]. There is a local optimal noise intensity of $D=0.1$, as shown in Fig. 4 right (D), at which the system output assisted by noise traces the suprathreshold input more correctly than at $D=0.002$. Beyond, too much noise will dominate the system output [see Fig. 4 right (e)], and the erroneous decoded digits are more frequent than at the optimal condition of $D=0.1$.

Figures 5 and 6 show the corresponding evolutions of the BER. Figures 5(a) and 5(b) show the BER as a function of the noise intensity D and the signal amplitude A/X_b at $T_p=0.9T_d$ and $T_p=1.05T_d$, respectively. Figure 6 shows the behavior of the BER vs noise intensity for representative values of A/X_b. We note the following.

(a) In Figs. 5(a), 6(a), and 6(c), at $T_p<T_d$, the BER presents a resonancelike behavior as the noise intensity increases. The minimal value of the BER is obtained at an optimal nonzero noise intensity.

(b) When $T_p>T_d$, the BER always starts from zero (at $D=0$) and then increases as the noise intensity increases, as shown in Figs. 5(b), 6(b), and 6(c). Upon further increase of the noise intensity, the BER reaches a local minimum for slightly suprathreshold amplitudes of A/X_b [see Figs. 5(b) and 6(b)]. However, this nonmonotonic behavior of the BER gradually vanishes for larger suprathreshold amplitudes of A/X_b at $T_p>T_d$ [see Figs. 5(b) and 6(c)]. For the slightly suprathreshold amplitude of A/X_b, the increase of the BER, as D just starts to rise above zero, is in accordance with the retardation observed in Fig. 4(c).

(c).Note that the residual ASR effect will not disappear for any suprathreshold input binary signals when $T_p<T_d$ [e.g., Fig. 5(a)]. As $T_p>T_d$, this form of ASR effect only exists in a limited range of A/X_b [e.g., Fig. 5(b)]. Therefore, this effect is referred to as the ''residual'' ASR.

We note that the residual ASR effect can also be measured by another performance measure, i.e., the channel capacity

$$C=1+P_e\log_2(P_e)+(1-P_e)\log_2(1-P_e), \qquad (5)$$

which is a monotone decreasing function of the BER [22]. The channel capacity can characterize the rate of information transfer in an efficient way [28,29]. The channel capacity will present the same resonancelike behaviors as the BER, with different resonance curve shapes. Hence, the BER is used in this paper without losing the general feature of the residual ASR effect.

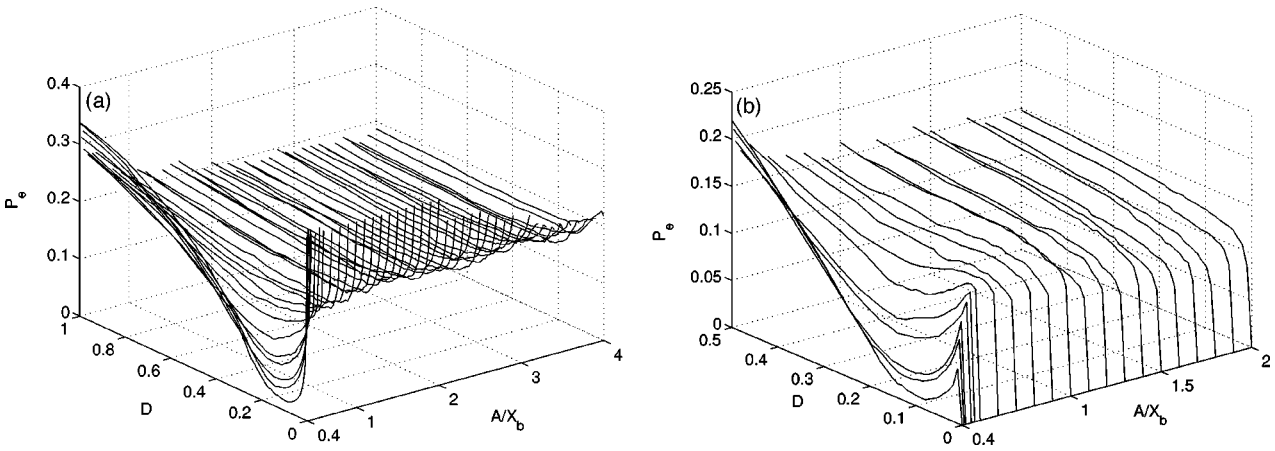

FIG. 5. Numerical results of the BER as a function of the noise intensity D (in units $\tau_a X_b^2$) and signal amplitudes A/X_b for the system with $\tau_a=1$ and $X_b=1$, at (a) $T_p=0.9T_d$; (b) $T_p=1.05T_d$. For different reduced amplitudes A/X_b, T_p are selected in terms of the corresponding values of T_d. The sampling time step $\Delta t=0.01\tau_a$.

Additionally, in this paper, the decision threshold ℓ is zero in accordance with the symmetrical characteristic of the information channel. We argue that residual ASR effect will also occur in signal detection with a decision threshold determined by a given false alarm probability [30]. Different thresholds will result in different system switching times. But if the pulse duration of the input signal is smaller than the corresponding system switching time, adding noise can also enhance the detection probability of the input signal through a similar noise-spurred response.

IV. A NONSTATIONARY PROBABILITY DENSITY MODEL

The qualitative understanding of the residual ASR effect in the preceding section is based on the comparison between the fast repetition time T_p of the input bit stream and the slow system switching time T_d measured in the absence of noise. We shall now attempt a more detailed theoretical analysis of the dynamics of Eq. (1), in the presence of both the binary input and the noise input, in order to seek a deeper understanding, at a more quantitative level, of the residual ASR effect.

A. System response time

The response of the system of Eq. (1), in the presence of both the binary input and the noise input, can be precisely described by solving the associated Fokker-Planck equation [31,32]. In each pulse duration T_p, the system of Eq. (1) is subjected to the constant signals $s(t)=\pm A$, i.e., wave forms $s_1(t)=+A$ or $s_2(t)=-A$, with an additional input Gaussian white noise $\eta(t)$. Under these conditions, the statistically equivalent description for the corresponding probability density $\rho(x,t)$ is governed by the Fokker-Planck equation

$$\tau_a \frac{\partial \rho(x,t)}{\partial t} = \left[\frac{\partial}{\partial x} V'(x) + \frac{D}{\tau_a} \frac{\partial^2}{\partial x^2} \right] \rho(x,t), \tag{6}$$

where $V'(x)=-x+x^3/X_b^2 \mp A$ and the Fokker-Planck operator is $L_{FP}=(\partial/\partial x)V'(x)+(D/\tau_a)(\partial^2/\partial x^2)$. $\rho(x,t)$ obeys the natural boundary conditions that it vanishes at large x for any t [31]. The steady-state solution of Eq. (6), for a permanent input at $+A$ or $-A$, is given by

$$\rho(x) = \lim_{t\to\infty} \rho(x,t) = C \exp\left[-\frac{\tau_a V(x)}{D} \right], \tag{7}$$

where C is the normalization constant [31].

Now, we will seek the nonstationary solution $\rho(x,t)$ of the Fokker-Planck equation, Eq. (6), in case of an input transition from $s(t)=-A$ to $s(t)=+A$, or conversely. This computation is performed in Appendix B. We show in Appendix B that the transition from the stationary density corresponding to $s(t)=-A$ to the stationary density corresponding to $s(t)=+A$, is dominated by an exponential temporal relaxation with reduced time constant $1/\lambda_1$. This allows us to deduce a response time $T_r=\tau_a/\lambda_1$ for the system, which is a measure of the time taken by the system to switch from one potential well to the other, when the binary input changes from $-A$ to $+A$ (or conversely), in the presence of noise. This system response time T_r have a similar qualitative interpretation as the system switching time T_d considered in the preceding section. But an essential advance is that T_r explicitly incorporates the influence of the input noise $\eta(t)$, while T_d conveys no such dependence. The study of T_r, as a function of the noise intensity D, then allows us to obtain a quantitative description of the residual ASR effect, or the effect of the spurring of the system by noise.

Figure 7 shows the system response time (dimensionless) $T_r/\tau_a=1/\lambda_1$ obtained from Appendix B, as a function of the noise intensity D and the signal amplitude A/X_b. At small A/X_b ($A/X_b>A_c/X_b\approx 0.38$), Fig. 7 shows a monotonic decay of T_r when D increases, expressing, as anticipated, that the switching dynamics of the system is accelerated as the noise level increases. At larger A/X_b, our theoretical results of Fig. 7 show a nonmonotonic action of the noise intensity D on T_r: At small D, the response time T_r starts to rise, revealing a tendency of the noise to slow down the dynam-

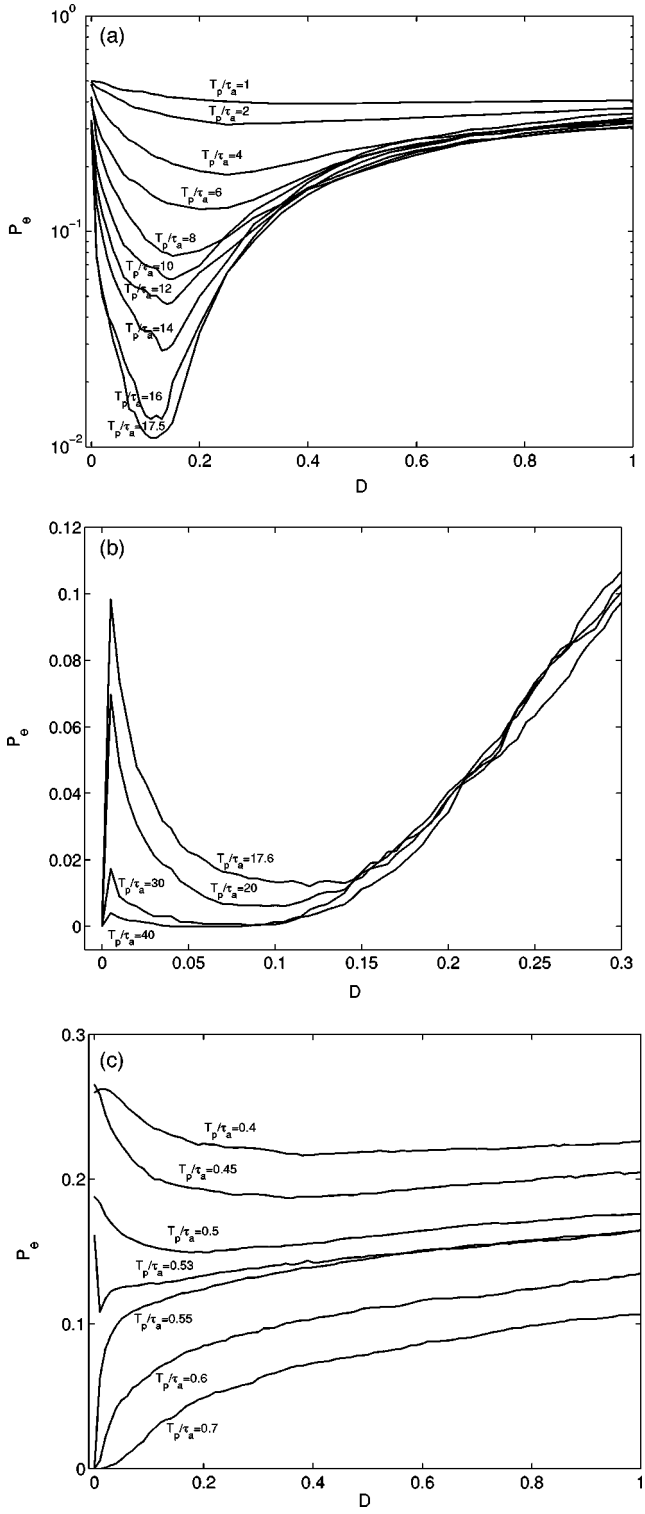

FIG. 6. Numerical results of the BER as a function of the noise intensity D (in units $\tau_a X_b^2$) for the system with $\tau_a=1$ and $X_b=1$. (a) $A/X_b=0.4$ at $T_p<T_d=17.5897$; (b) $A/X_b=0.4$ at $T_p>T_d$; (c) $A/X_b=3$ at $T_p<T_d=0.53\,102$ and $T_p>T_d$. The sampling time step $\Delta t=0.01\tau_a$.

ics; yet, this unexpected behavior takes place in a narrow range for D, then to give way to the expected decay of T_r as D is further increased. Therefore, the standard behavior that is evidenced in Fig. 7 is the reduction of the response time T_r

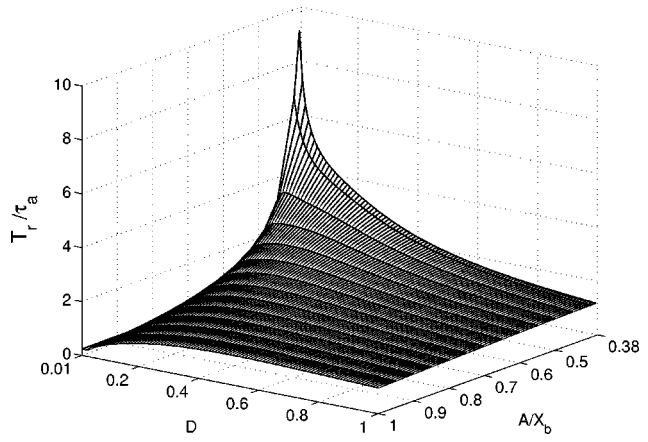

FIG. 7. Theoretical results of the system response time T_r/τ_a vs A/X_b and D (in units $\tau_a X_b^2$).

as the noise level D increases, i.e., the switching dynamics accelerated by noise.

The reduction of the response time T_r with increasing D is only half of the mechanism at work to deliver the nonmonotonic evolution of the BER as shown in Figs. 5 and 6. The other important part of the mechanism is that, as the noise level increases, although it accelerates the switching dynamics of the system, it also enhances the fluctuations that $x(t)$ undergoes once it has reached one potential well or the other. The accelerated switching dynamics is favorable, while the enhanced fluctuations are detrimental, to the correct transmission of the binary data. This two parts played by the noise (acceleration of the switching dynamics between wells, and enhancement of the fluctuations inside the wells) result in the nonmontonic evolutions of the BER shown in Figs. 5 and 6.

To take further our theoretical description that gave us a dependence of T_r with D, we now proceed to obtain a theoretical expression for the BER to be studied as a function of D.

B. A theoretical nonstationary probability density model

In Appendix B, the nonstationary density $\rho(x,t)$ for an input transition from $s(t)=-A$ to $s(t)=+A$ (or conversely) is approximated with the two first terms from its asymptotic representation of Eq. (B11), as

$$\rho[x,t|s(t)=\pm A]\simeq\rho[x|s(t)=\pm A]+\{\rho[x|s(t)=\mp A]-\rho[x|s(t)=\pm A]\}\times\exp(-t/T_r), \tag{8}$$

where $\rho[x|s(t)=\pm A]=C\exp[-\tau_a V(x)/D]$ are the steady-state solutions given in Eq. (7). In Eq. (8), when $t=0$, the term $\exp(-t/T_r)=1$ and $\rho[x,t|s(t)=\pm A]$ starts with the initial condition of $\rho[x|s(t)=\mp A]$. As $t\to+\infty$, the term $\exp(-t/T_r)=0$, and $\rho[x,t|s(t)=\pm A]$ tends to the stationary condition of $\rho[x|s(t)=\pm A]$.

At the output, the decision for decoding the binary digits, as introduced in Sec. II, is to compare the sampled values of $x_j=x(jT_p)$ to the threshold $\ell=0$. Based on our approxima-

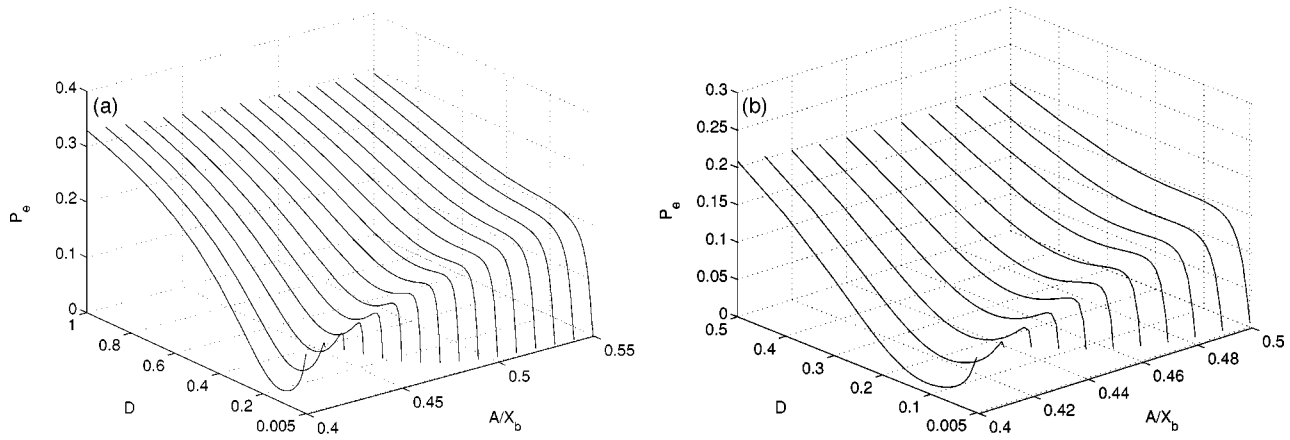

FIG. 8. Theoretical results of the BER based on the nonstationary probability density model, for the system with $\tau_a=1$ and $X_b=1$, for different amplitudes of A/X_b at (a) $T_p=0.9T_d$; (b) $T_p=1.05T_d$. Note that this theory of Eq. (9) cannot be evaluated at $D=0$.

tion of the nonstationary probability density of Eq. (8), the BER of Eq. (2) can be theoretically expressed as

$$P_e=\frac{1}{2}[P(1|0)+P(0|1)]$$
$$=\frac{1}{2}\left[\int_0^{+\infty}\rho[x,T_p|s(t)=-A]dx+\int_{-\infty}^{0}\rho[x,T_p|s(t)=+A]dx\right]. \quad (9)$$

When Eq. (8) is introduced in Eq. (9), it is visible that the term $\exp(-T_p/T_r)$ should satisfy the condition of $\exp(-T_p/T_r)\leqslant 1/2$, i.e., T_p should not be sufficiently small compared to T_r. It is in this case that the BER falls below 1/2, and that effective binary transmission can take place [22]. The following quantitative results which are presented in Figs. 8 and 9 are all calculated in this regime where $\exp(-T_p/T_r)\leqslant 1/2$.

Figures 8 and 9 illustrate the theoretical results of the BER of Eq. (9) as a function of the noise intensity D and the input amplitude A/X_b. As visible, these theoretical results also show the effect of residual ASR in suprathreshold signal transmission, and they are in good qualitative agreement with the simulation results of Figs. 5 and 6. There are some discrepancies at the quantitative level, because our theoretical model is an approximation. By comparing Fig. 9 to the numerical results of Fig. 6, it can be seen that the theory especially fits well when T_p/τ_a is large. Overall, our theoretical model, although approximate, captures well the double role played by the noise, both in accelerating the switching dynamics between wells while enhancing the fluctuations inside the wells, this resulting in a nonmonotonic evolution of the BER.

V. CONCLUSION

A different form of ASR, residual ASR phenomenon, has been demonstrated in a *single* bistable dynamic system driven by a suprathreshold binary signal. An essential feature of residual ASR is given by the competition between the signal pulse duration and the system switching time. The noise essentially plays a constructive role by accelerating the switching dynamics of a slow system for a more efficient transmission of a fast input.

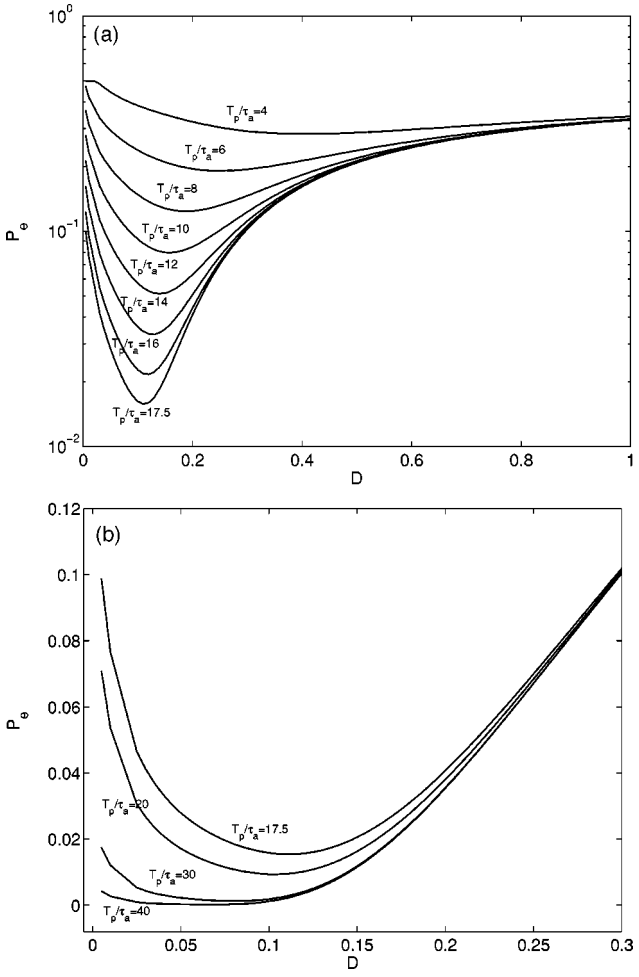

FIG. 9. Theoretical results of the BER based on the nonstationary probability density model for the system with $\tau_a=1$, $X_b=1$, $A/X_b=0.4$ at (a) $T_p<T_d$; (b) $T_p>T_d$. Note that this theory of Eq. (9) cannot be evaluated at $D=0$.

Residual ASR is a nontrivial effect and raises other related interesting lines of investigation. For instance, the neurophysiological sensory system responses to some fast stimuli in the background of noise, with a non-negligible dynamic system characteristic time. We also argue that the residual ASR effect can be demonstrated in bistable electronic or optical experiments transmitting suprathreshold input signals [3,12]. These subjects are very promising and currently under study.

ACKNOWLEDGMENT

F. Duan acknowledges financial support of la Région des Pays de la Loire, France.

APPENDIX A: THEORETICAL SOLUTION OF THE SYSTEM SWITCHING TIME

The cubic equation $x-x^3/X_b^2+A=0$ has one real root x_+ and two conjugate complex roots x_1 and x_2 as

$$x_+=-\frac{2^{1/3}q}{3p^{1/3}}+\frac{p^{1/3}}{3\times 2^{1/3}},$$

$$x_{1,2}=\frac{(1\pm i\sqrt{3})q}{3\times 2^{2/3}p^{1/3}}-\frac{(1\mp i\sqrt{3})p^{1/3}}{6\times 2^{1/3}}, \tag{A1}$$

where $q=-3X_b^2$, $p=-r+\sqrt{4q^3+r^2}$, and $r=-27AX_b^2$. Next, we can expand [35]

$$\frac{1}{x-x^3/X_b^2+A}=\frac{C_1}{x-x_+}+\frac{C_2}{x-x_1}+\frac{C_3}{x-x_2}, \tag{A2}$$

with

$$C_1=-C_2-C_3,\quad C_2=\frac{-X_b^2}{(x_+-x_1)(x_2-x_1)},$$

$$C_3=\frac{-X_b^2}{(x_+-x_2)(x_1-x2)}. \tag{A3}$$

Thus, from a initial position x_0 to the end position x, the system switching time T_d reads

$$\frac{T_d}{\tau_a}=\int_{x_0}^{x}\frac{dx'}{x'-x'^3/X_b^2+A}=C_1\ln\left[\frac{x-x_+}{x_0-x_+}\right]+C_2\ln\left[\frac{x-x_1}{x_0-x_1}\right]+C_3\ln\left[\frac{x-x_2}{x_0-x_2}\right]. \tag{A4}$$

Then, Eq. (4) is derived.

APPENDIX B: SYSTEM RESPONSE TIME AND NONSTATIONARY PROBABILITY DENSITY MODEL

The following approximate method for obtaining the system response time has been discussed in Ref. [32]. Here we give a simple demonstration for the bistable dynamic system described by Eq. (1). This method is also applicable for other nonlinear systems analyzed in Refs. [5,33] with different potential functions. Next, based on the system response time, a nonstationary probability density model is established in this paper.

1. System response time

In Eq. (6), the Fokker-Planck operator $L_{FP}=(\partial/\partial x)V'(x)+(D/\tau_a)\partial^2/\partial x^2$ is not a Hermitian operator [31]. We rescale the variables as

$$\tau=t/\tau_a,\quad y=x/\sqrt{D/\tau_a},\quad \overline{X_b}=X_b/\sqrt{D/\tau_a},$$

$$\overline{A}=A/\sqrt{D/\tau_a}, \tag{B1}$$

Eq. (6) becomes

$$\frac{\partial\rho(y,\tau)}{\partial\tau}=\left[\frac{\partial}{\partial y}V'(y)+\frac{\partial^2}{\partial y^2}\right]\rho(y,\tau), \tag{B2}$$

where $V'(y)=-y+y^3/\overline{X_b^2}\mp\overline{A}$. The steady-state solution of Eq. (B2) is given by

$$\rho(y)=\lim_{\tau\to\infty}\rho(y,\tau)=C\exp[-V(y)], \tag{B3}$$

where C is the normalization constant. A separation ansatz for $\rho(y,\tau)$ [31],

$$\rho(y,\tau)=u(y)\exp\left[-\frac{V(y)}{2}\right]\exp(-\lambda\tau), \tag{B4}$$

leads to

$$Lu=-\lambda u, \tag{B5}$$

with a Hermitian operator $L=(\partial^2/\partial y^2)-[\frac{1}{4}V'^2(y)-\frac{1}{2}V''(y)]$. The functions $u(y)$ are eigenfunctions of the operator L with the eigenvalues λ. Multiplying both sides of Eq. (B5) by $u(y)$ and integrating it, yields

$$\lambda=\frac{\int_{-\infty}^{+\infty}\left\{u'^2(y)+u^2(y)\left[\frac{1}{4}V'^2(y)-\frac{1}{2}V''(y)\right]\right\}dy}{\int_{-\infty}^{+\infty}u^2(y)dy}, \tag{B6}$$

where eigenfunctions $u(y)$ satisfy the boundary conditions of $\lim_{y\to\pm\infty}u(y)=0$ and $\lim_{y\to\pm\infty}u'(y)=0$. The eigenvalue problem of Eq. (B5) is then equivalent to the variational problem consisting in finding the extremal values of the right side of Eq. (B6) [31,32]. The minimum of this expression is then the lowest eigenvalue $\lambda_0=0$, corresponding to the steady-state solution of Eq. (B3) [31]. We adopt here eigenfunctions $u(y)=p(y)\exp[-V(y)/2]$ and $p(y)\neq 0$, Eq. (B6) becomes

$$\lambda = \frac{\int_{-\infty}^{+\infty} \left\{ p'^2(y) + \frac{1}{2} p^2(y) V'^2(y) - \frac{1}{2} [V'(y) p^2(y)]' \right\} \exp[-V(y)] dy}{\int_{-\infty}^{+\infty} p^2(y) \exp[-V(y)] dy}. \quad \text{(B7)}$$

Since

$$\int_{-\infty}^{+\infty} [V'(y)p^2(y)]' \exp[-V(y)] dy = V'(y)p^2(y) \times \exp[-V(y)]|_{-\infty}^{+\infty} + \int_{-\infty}^{+\infty} p^2(y) V'^2(y) \exp[-V(y)] dy = \int_{-\infty}^{+\infty} p^2(y) V'^2(y) \exp[-V(y)] dy,$$

Eq. (B7) can be rewritten as

$$\lambda = \frac{\int_{-\infty}^{+\infty} p'^2(y) \exp[-V(y)] dy}{\int_{-\infty}^{+\infty} p^2(y) \exp[-V(y)] dy}. \quad \text{(B8)}$$

Assume $p(y) = d_0 + d_1 y + \cdots + d_n y^n$ and the order n is an integer, we obtain

$$([K] - \lambda[M])\{d\} = 0, \quad \text{(B9)}$$

with eigenvectors $\{d^i\} = [d_0^i, d_1^i, \ldots, d_n^i]$ corresponding to eigenvalues $\{\lambda\} = [\lambda_0, \lambda_1, \ldots, \lambda_n]$ for $i = 0,1,\ldots,n$. The integer n is not increased in the iterative process until the preceding values of λ_i approximate the next ones within the tolerance error. The elements of matrices $[M]$ and $[K]$ are

$$m_{ij} = \int_{-\infty}^{+\infty} y^{i+j} \exp[-V(y)] dy > 0,$$

$$k_{ij} = \int_{-\infty}^{+\infty} ij y^{i+j-2} \exp[-V(y)] dy \geqslant 0,$$

where $i, j = 0,1,\ldots,n$. The matrix $[M]$ is positive definite and the matrix $[K]$ is semipositive definite. The minimal eigenvalue λ_0 is zero. The inverse of minimal positive eigenvalue λ_1 describes the main time of the system tending to the steady state solution of Eq. (B3), what we call the system response time. Note the time scale transformation in Eq. (B1), the minimal positive eigenvalue should be λ_1/τ_a and the real system response time is $T_r = \tau_a/\lambda_1$. The reduced dimensionless system response time is then $T_r/\tau_a = 1/\lambda_1$.

2. Nonstationary probability density model

From Eq. (B9), we can obtain the eigenfunctions $u_i(y) = p_i(y)\exp[-V(y)/2]$ corresponding to the eigenvalue λ_i for $i = 0,1,\ldots,n$, where $p_i(y) = d_0^i + d_1^i y + \cdots + d_n^i y^n$. The eigenvectors $\{d^i\} = [d_0^i, d_1^i, \ldots, d_n^i]$ are normalized. Because L is a Hermitian operator, eigenfunctions $u_i(y)$ and $u_j(y)$ are orthogonal

$$\int_{-\infty}^{+\infty} u_i(y) u_j(y) dy = \delta_{ij}, \quad \text{(B10)}$$

where $i, j = 0,1,\ldots,n$. $\rho(y,\tau)$ can be expanded, according to eigenfunctions $u_i(y)$ and eigenvalues λ_i, as

$$\rho(y,\tau) = \sum_{i=0}^{n} C_i u_i(y) \exp\left[-\frac{V(y)}{2}\right] \exp[-\lambda_i \tau], \quad \text{(B11)}$$

where C_i are normalization constants. In this paper, we take an approximate expression of $\rho(y,\tau) \simeq \Sigma_{i=0}^{1} C_i u_i(y) \exp[-V(y)/2]\exp[-\lambda_i \tau]$ instead of Eq. (B11). Then, if the preceding input signal is $s(t) = \mp A$ and the next one is $s(t) = \pm A$, a simple nonstationary probability density model is derived as

$$\rho[x,t|s(t) = \pm A] \simeq \rho[x|s(t) = \pm A] + \{\rho[x|s(t) = \mp A] - \rho[x|s(t) = \pm A]\} \exp(-t/T_r), \quad \text{(B12)}$$

with the initial and stationary conditions

$$\rho[x, t = 0|s(t) = \pm A] = \rho[x|s(t) = \mp A],$$

$$\rho[x, t = +\infty|s(t) = \pm A] = \rho[x|s(t) = \pm A].$$

Here, $\rho[x|s(t) = \pm A] = C \exp[-\tau_a V(x)/D]$ are the steady-state solutions given in Eq. (7), and $V(x) = -x^2/2 + x^4/(4X_b^2) \mp Ax$ correspond to the constant inputs $s(t) = \pm A$, respectively. This kind of nonstationary solution of $\rho[x,t|s(t) = \pm A]$ can be further developed into the case of $\rho(y,\tau) \simeq \Sigma_{i=0}^{n} C_i u_i(y) \exp[-V(y)/2]\exp[-\lambda_i \tau]$ for $n \geqslant 2$ [34]. The remaining open question is the influence of the cutting terms on the accuracy of the nonstationary probability density function.

[1] R. Benzi, A. Sutera, and A. Vulpiani, J. Phys. A **14**, L453 (1981).

[2] R. Benzi, G. Parisi, A. Sutera, and A. Vulpiani, Tellus **34**, 10 (1982).

[3] L. Gammaitoni, P. Hänggi, P. Jung, and F. Marchesoni, Rev. Mod. Phys. **70**, 233 (1998).

[4] F. Moss, D. Pierson, and D. O'Gorman, Int. J. Bifurcation Chaos Appl. Sci. Eng. **4**, 1383 (1994).

[5] A.R. Bulsara and L. Gammaitoni, Phys. Today **49**, 39 (1996).
[6] J.J. Collins, C.C. Chow, and T.T. Imhoff, Phys. Rev. E **52**, R3321 (1995).
[7] C. Heneghan *et al.*, Phys. Rev. E **54**, R2228 (1996).
[8] A.R. Bulsara and A. Zador, Phys. Rev. E **54**, R2185 (1996).
[9] D. DeWeese and W. Bialek, Nuovo Cimento D **17**, 733 (1995).
[10] J.E. Levin and J.P. Miller, Nature (London) **380**, 165 (1996).
[11] X. Pei, L. Wilkens, and F. Moss, Phys. Rev. Lett. **77**, 4679 (1996).
[12] F. Apostolico, L. Gammaitoni, F. Marcheson, and S. Santucci, Phys. Rev. E **55**, 36 (1997).
[13] L. Gammaitoni and A.R. Bulsara, Phys. Rev. Lett. **88**, 1 (2002).
[14] N.G. Stocks, Phys. Rev. Lett. **84**, 2310 (2000).
[15] N.G. Stocks, Phys. Lett. A **279**, 308 (2001).
[16] N.G. Stocks, Phys. Rev. E **63**, 1 (2001).
[17] N.G. Stocks and R. Mannella, Phys. Rev. E **64**, 1 (2001).
[18] R.P. Morse and E.F. Evans, Nat. Med. **2**, 928 (1996).
[19] R.P. Morse and E.F. Evans, Hear. Res. **133**, 120 (1999).
[20] M.J. Chacron, A. Longtin, M. St-Hilaire, and L. Maler, Phys. Rev. Lett. **85**, 1576 (2000).
[21] L. Gammaitoni, F. Marchesoni, E. MenichellaSaetta, and S. Santucci, Phys. Rev. Lett. **71**, 3625 (1993).
[22] J.G. Proakis, *Digital Communications*, 3rd ed. (McGraw-Hill, New York, 1995).
[23] S. Barbay, G. Giacomelli, and F. Marin, Phys. Rev. Lett. **85**, 4652 (2000).
[24] S. Barbay, G. Giacomelli, and F. Marin, Phys. Rev. E **63**, 1 (2001).
[25] X. Godivier and F. Chapeau-Blondeau, Int. J. Bifurcation Chaos Appl. Sci. Eng. **8**, 581 (1998).
[26] F. Duan and B. Xu, Int. J. Bifurcation Chaos Appl. Sci. Eng. **13**, 411 (2003).
[27] T.C. Gard, *Introduction to Stochastic Differential Equations* (Marcel Dekker, New York, 1998).
[28] F. Chapeau-Blondeau, Phys. Rev. E **55**, 2016 (1997).
[29] L.B. Kish, G.P. Harmer, and D. Abbott, Fluct. Noise Lett. **1**, L13 (2001).
[30] M.E. Inchiosa and A.R. Bulsara, Phys. Rev. E **53**, R2021 (1996).
[31] H. Risken, *The Fokker-Planck Equation: Methods of Solution and Applications*, Springer Series in Synergetics Vol. 18, 2nd ed. (Springer-Verlag, Berlin, 1989).
[32] B. Xu, F. Duan, R. Bao, and J. Li, Chaos, Solitons Fractals **13**, 633 (2002).
[33] J. Li, R. Bao, and B. Xu, Physica A **323**, 249 (2003).
[34] B. Xu (private communication).
[35] D. Rousseau (unpublished).